

A Label-Free Immunoassay Based Upon Localized Surface Plasmon Resonance of Gold Nanorods

Kathryn M. Mayer,[†] Seunghyun Lee,[‡] Hongwei Liao,[‡] Betty C. Rostro,[†] Amaris Fuentes,[†] Peter T. Scully,[†] Colleen L. Nehl,[†] and Jason H. Hafner^{†,‡,*}

[†]Department of Physics & Astronomy and [‡]Department of Chemistry, Rice University, Houston, Texas 77005

Gold and silver nanoparticles exhibit localized surface plasmon resonances (LSPR) at visible and near-infrared frequencies, leading to sharp peaks in their spectral extinction.¹ The dependence of the resonance condition on the local dielectric environment enables a simple form of molecular sensing in which analyte binding to the nanoparticles surface causes a shift in the spectral extinction peak.² LSPR sensing is therefore the nanoparticle analogue of surface plasmon resonance sensing (SPR), which similarly monitors the resonance condition for surface plasmons in thin gold films.³ SPR is a powerful surface analytical technique since it can detect submonolayer quantities of analyte at the gold film surface. Furthermore, since SPR measures an inherent property of the analyte, it does not require further labeling or chemical amplification. SPR can therefore measure dynamic processes in real time such as binding kinetics of biomolecular interactions, rather than simply providing the end-points. These properties have led to widespread use of SPR in the study of biomolecular interactions, as well as antibody screening for diagnostic and therapeutic applications.^{4,5} However, despite its analytical capabilities, SPR is not widely used in clinical immunoassays or other nonresearch applications owing to the complexity of the optical instrumentation and the need for precise temperature control. It has been suggested that LSPR sensing with nanoparticle substrates will preserve the virtues of SPR but greatly broaden the scientific and technological applications, since LSPR sensing is based on a simple optical extinction measurement, is not temperature sensitive, and requires only common laboratory equipment.⁶ Furthermore, nanoparticles have a highly local-

www.acsnano.org

ABSTRACT Robust gold nanorod substrates were fabricated for refractive index sensing based on localized surface plasmon resonance (LSPR). The substrate sensitivity was 170 nm/RIU with a figure of merit of 1.3. To monitor biomolecular interactions, the nanorod surfaces were covered with a self-assembled monolayer and conjugated to antibodies by carbodiimide cross-linking. Interactions with a specific secondary antibody were monitored through shifts in the LSPR spectral extinction peak. The resulting binding rates and equilibrium constant were in good agreement with literature values for an antibody–antigen system. The nanorod LSPR sensors were also shown to be sensitive and specific. These results demonstrate that given a sufficiently stable nanoparticle substrate with a well defined chemical interface, LSPR sensing yields similar results to the surface plasmon resonance technique, yet with much simpler instrumentation.

KEYWORDS: gold nanorod · biosensor · immunoassay · localized surface plasmon resonance · SPR · nanobiotechnology · nanophotonics

ized LSPR sensing volume which eliminates the need to trap the interacting molecules of interest in a polymer matrix to enhance the signal, as is often done in SPR measurements.

LSPR sensing has evolved through the research of several groups over the past decade. The principle was first demonstrated in 1998 with antibody-conjugated gold nanoparticles in solution.⁷ To mitigate spurious spectral shifts due to aggregation, nanoparticles were conjugated to monoclonal antibodies specific for a single epitope on the target ligand. However, to completely remove the possibility of aggregation, others have worked with nanoparticles bound to a transparent substrate, as demonstrated with silver nanotriangles created by nanosphere lithography,⁸ and gold colloid films on glass.⁹ Since these initial studies, there have been many reports on the technique^{10–29} including demonstrations of multiplexing,^{20,30} the detection of medically relevant analytes in clinical samples,³¹ and fiber-based sensors.^{10,13}

Despite these successes, LSPR sensing is still not nearly as prevalent as SPR. Thus far,

See the accompanying Perspective by Odom and Nehl on p 612.

*Address correspondence to hafner@rice.edu

Received for review November 18, 2007 and accepted February 11, 2008.

Published online February 22, 2008.
10.1021/nn7003734 CCC: \$40.75

© 2008 American Chemical Society

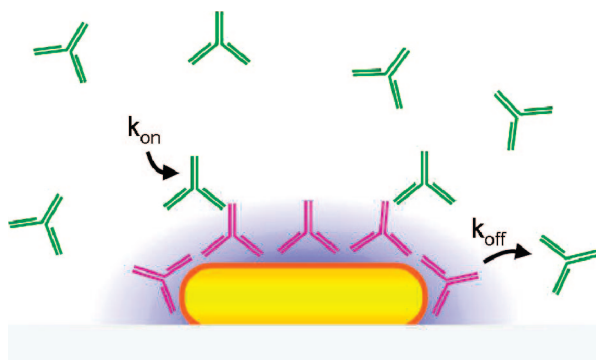


Figure 1. Schematic of the nanorod-based immunoassay. The nanorods are fixed to a glass surface *via* an APTES monolayer, and then coated with a self-assembled monolayer to which the capture antibody is coupled by carbodiimide cross-linking. The substrate is exposed to antigen (in this case secondary antibodies) and the binding is monitored *via* real-time absorption spectra.

biomolecular LSPR sensing studies have focused on biotin/streptavidin and antigen/antibody interactions, with a few exceptions.^{14,16,22,32} All reports find a red shift as the ligand binds to the nanoparticles, but most do not observe the correct equilibrium binding constant (K_{eq}) when the interaction is studied in detail. A few reports have measured the correct K_{eq} value for antigen/antibody interactions,^{12,20} but these were from endpoint assays rather than kinetics. Here we describe real-time analysis of antibody–antigen interactions by LSPR sensing with self-assembled gold nanorod substrates (Figure 1).³³ Through careful control of the substrate surface chemistry, we demonstrate the first successful measurement of binding constants by LSPR sensing.

RESULTS AND DISCUSSION

The gold nanorods for this report were produced by seed-mediated, surfactant directed synthesis,^{34,35} which has been widely applied to generate homogeneous gold nanorods in high yield with LSPR resonances in the visible and near-infrared. Slight variations in the reactant ratios yield a variety of other anisotropic shapes.³⁴ However, further chemical manipulation of these nanoparticles is somewhat more complicated than that of classic citrate-stabilized gold colloid.³⁶ In surfactant directed synthesis, the CTAB acts as both the source of anisotropic growth and the stabilizer.³⁷ The 100 mM CTAB is thought to form a cationic bilayer around the nanoparticles, yet is clearly bound in a weak manner since a reduction of the CTAB concentration to below 1 mM causes aggregation. We previously reported a simple method to displace the CTAB stabilizer with a thiol terminated PEG.³³ Once PEGylated, the nanorods can be transferred to solutions devoid of PEG or other stabilizers. PEGylation allowed bioconjugation of the nanorods in solution and processing of nanorods into well-ordered films. Figure 2 displays such a film, demonstrating the uniformity of deposition.

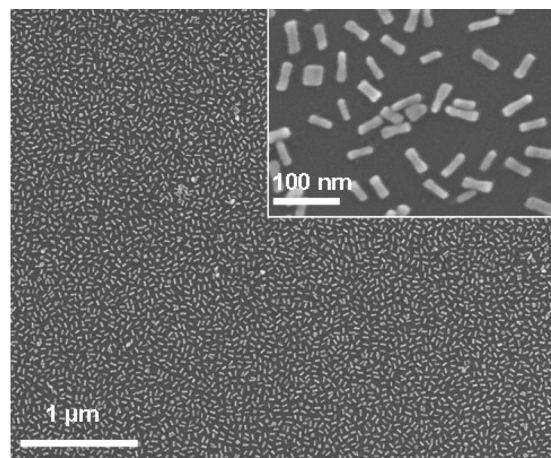


Figure 2. Scanning electron microscopy of films of gold nanorods. The coverage is uniform over large areas of the substrate. The individual nanorods are about 15 nm in diameter and 50 nm long.

Our initial attempts to use the PEGylation and bioconjugation protocols cited above for LSPR sensing produced shifts in response to binding, but did not yield the correct equilibrium binding constant for antigen/antibody interactions. Therefore, we adopted a surface chemistry based on self-assembled monolayers (SAMs).³⁸ First, the nanorod substrates were treated with oxygen plasma to remove the PEG and expose a clean gold surface. (The plasma presumably does not etch the APTES linkages holding the nanorods to the glass substrate.) Once cleaned, mixed SAMs of mercaptohexadecanoic acid and mercaptoundecanol were formed on the nanoparticles. Since SAMs on nanoparticles larger than 4 nm in diameter have been reported to exhibit behavior similar to those on planar surfaces,³⁹ the nanorods can be thought of as planar SPR surfaces in terms of their surface chemistry.

The sensitivity of the SAM-coated nanorod substrates to changes in the refractive index was checked by measuring the LSPR spectral extinction in air, water, ethanol (not shown), and formamide (Figure 3). This yielded a refractive index sensitivity of 170 nm per refractive index unit (RIU). While this sensitivity is not exceedingly high as compared to those in other reports,⁴⁰ the resonances are fairly narrow with a full width of 125 nm in water. The resulting figure of merit (sensitivity/line width)⁴¹ for these sensors is 1.3, which is similar to other reports on nanoparticle ensembles.⁴⁰

The nanorod substrates were tested as LSPR sensors in the flow cell by activating the carboxylic acid groups on the SAM *via* carbodiimide chemistry.³⁶ Rabbit IgG was coupled to the SAM to serve as a capture antibody, so that the binding of specific and nonspecific antibodies could be studied. The LSPR peak wavelength throughout such a reaction is displayed in Figure 4. First, the peak wavelength was allowed to stabilize against solvent annealing under a flowing buffer (not shown).⁴² Exposure of the activated carboxy-terminal

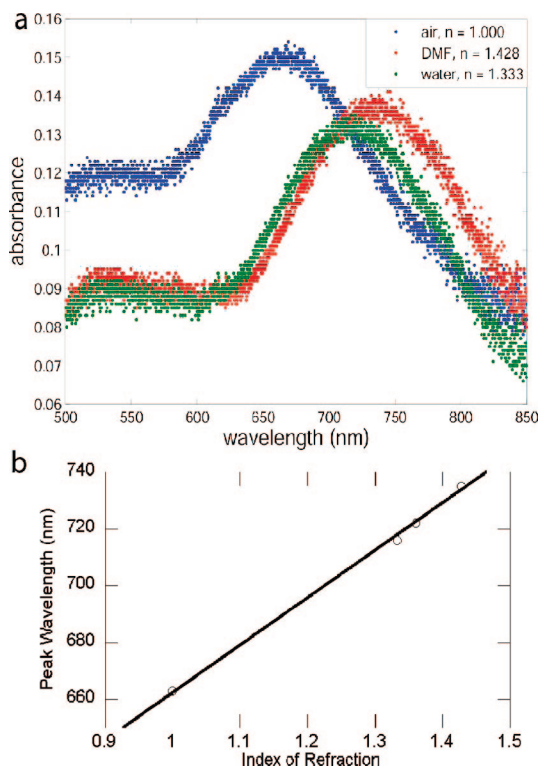


Figure 3. Characterization of the LSPR sensitivity to refractive index of the nanorod films: (a) Spectra of a nanorod film in three dielectric media. (b) The slope of the line yields a sensitivity of 170 nm/RIU.

nanorod SAM substrate to rabbit IgG produced the expected red shift of the LSPR peak wavelength due to IgG binding. The subsequent blue shift occurred during rinsing and was likely due to the removal of physisorbed rabbit IgG. Exposure to 30 nM goat antirabbit IgG caused a further red shift as the specific secondary antibody bound the capture antibody on the sensor.

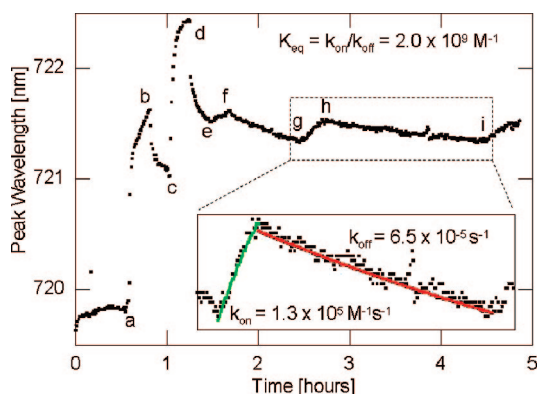


Figure 4. Immunoassay with kinetic data fits. The peak absorbance wavelength was measured *versus* time as the various solutions flowed over the substrate in a continuous experiment. Initially, the substrate was under a pH 6.1 buffer solution. At step a the substrate was exposed to a mixture of NHS and EDC, activating the SAM for protein binding. At step b, the substrate was rinsed with pH 6.1 buffer. At step c, rabbit immunoglobulin (IgG) was introduced. At step d, the substrate was rinsed with pH 7.6 buffer. At step e, it was exposed to 30 nM goat antirabbit IgG. At step f, it was again rinsed in pH 7.6 buffer. At steps g through i, these final steps were repeated twice more.

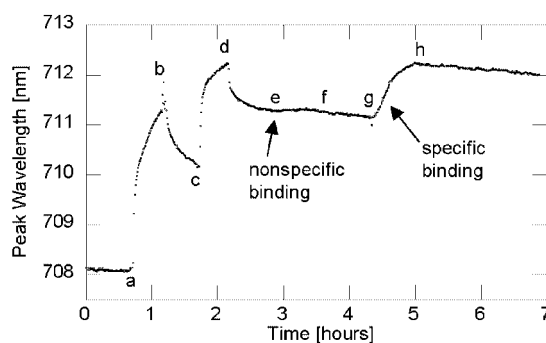


Figure 5. Demonstration of sensor specificity. Steps a through d are as in Figure 4. In step e, the substrate was exposed to 10 nM goat antimouse IgG, a nonspecific secondary antibody to the rabbit IgG. The binding is extremely weak. Step f is a buffer rinse. In step g, the substrate was exposed to 10 nM goat antirabbit IgG, and strong, specific binding was seen. Step h is a buffer rinse.

Then, the substrate was rinsed and unbinding of the secondary antibody was monitored *via* a blue shift. The final goat antirabbit IgG step was repeated three times to demonstrate substrate stability. The on and off rates for antibody binding were fit with a standard 1:1 binding model⁴³ which yielded the following:

$$k_{\text{off}} = 6.5 \times 10^{-5} \text{ s}^{-1}$$

$$k_{\text{on}} = 1.3 \times 10^5 \text{ M}^{-1} \text{ s}^{-1}$$

resulting in an equilibrium constant:

$$K_{\text{eq}} = 2.0 \times 10^9 \text{ M}^{-1}$$

This is a typical equilibrium constant for an antigen-antibody interaction,⁴³ and is the first measurement of the equilibrium constant from kinetic rates by LSPR sensing. This measurement was repeated several times, yielding equilibrium constants between $2 \times 10^8 \text{ M}^{-1}$ and $2 \times 10^9 \text{ M}^{-1}$. The additional data and fits can be found in the Supporting Information. The rates presented here match well to those observed for antigen-antibody binding in SPR.

Figure 5 illustrates a similar assay that tests the nanorod LSPR sensor's specificity. The nanorod conjugation with rabbit IgG was carried out exactly as described above, but the substrate was then exposed to 10 nM goat antimouse IgG as an analyte. As expected, there was very little binding of the nonspecific secondary antibody. When the specific secondary antibody was added in a subsequent step, significant binding was observed. This explicit demonstration confirms that the LSPR sensor retains the specificity of the capture antibody.

In addition, the detection sensitivity was measured. In Figure 6, the nanorod conjugation with rabbit IgG is again the same as in Figure 4, but in this case, the concentration of goat antirabbit IgG was raised in subse-

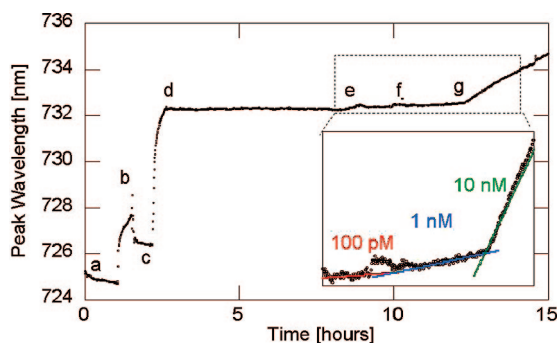


Figure 6. Test of sensor sensitivity. Steps a through d are as in Figure 4. In step e, the specific antibody (goat-anti rabbit IgG) was added at a concentration of 100 pM. The concentration was increased to 1 nM (at f) and 10 nM (at g). The inset shows linear fits to the binding curve.

quent steps. When the antibody was added at a concentration of 100 pM, there was no measurable response. When the concentration was increased to 1 nM, the peak began to redshift, with a slope of 0.076 ± 0.005 nm/hour. When the concentration was again increased to 10 nM, the slope, which should be proportional to concentration (to first order), also increased 10-fold, to 0.76 ± 0.007 nm/hour. From this, we found that the limit of detection of this sensor over a reasonable time scale is about 1 nM.

Figure 7 illustrates the relationship between the LSPR shift due to the capture antibody binding and the LSPR shift due to analyte antibody binding over several experiments using different substrates. The linear

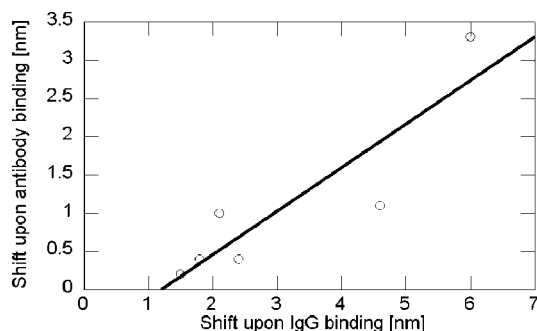


Figure 7. Comparison of LSPR shifts upon initial protein binding and specific antibody binding.

MATERIALS AND METHODS

Gold Nanorod Synthesis. Gold nanorods were prepared as described previously,³⁴ but the procedure was scaled up to increase the quantity.³³ All solutions were prepared fresh for each synthesis, except for the hydrogen tetrachloroaurate(III) (Sigma, no. 520918), which was prepared as a 28 mM stock solution from a dry ampule and stored in the dark. An aliquot of the stock solution was diluted to 10 mM immediately before use. Gold seed particles were prepared by adding 250 μ L of 10 mM hydrogen tetrachloroaurate(III) to 7.5 mL of 100 mM cetyltrimethylammonium bromide (CTAB) (Sigma, #H9151) in a plastic tube with brief, gentle mixing by inversion. Next, 600 μ L of 10 mM sodium borohydride (Acros, #18930) was prepared from DI water chilled to 2–8 °C in a refrigerator and added to the seed solution immediately after preparation, followed by mixing by inversion

relationship demonstrates that the results are reproducible and consistent from experiment to experiment, and that the variation in signal is most likely due to variation in the yield of capture antibody conjugation.

Most recent work on LSPR sensors has focused on maximizing the dielectric sensitivity by optimizing the nanoparticle shape.^{40,44–46} While this is certainly advantageous, it is not a complete solution to extending LSPR applications in science and technology. More significant issues are the stability and availability of the sensor substrates, their chemical interface with the analyte, and the need for quantitative dynamic measurements. Here we have addressed these issues by fabricating LSPR substrates based on chemically synthesized gold nanorods with no lithographic steps and by exploiting standard techniques in self-assembly and bioconjugate chemistry. The resulting substrates are highly stable, as seen in the >15 h experiment in Figure 6. Also, the substrates can be plasma cleaned and reused, with some having undergone >20 such cycles in our laboratory. Although the nanorod substrates are not as sensitive as some other LSPR systems and geometries, their performance is comparable to dynamic SPR measurements in immunoassays. Such immunoassays may prove to be a significant application of LSPR sensing given the need for broadly available high throughput screening in fields such as proteomics, systems biology, and in vitro diagnostics.

CONCLUSIONS

Gold nanorod LSPR sensor substrates were fabricated by self-assembly for the study of biomolecular interactions. Through careful control of their surface chemistry, the nanorods were conjugated with capture antibodies which enabled immunospecific detection of secondary antibodies. Correct binding kinetics were measured, thus demonstrating that the nanorod LSPR sensor can monitor real-time dynamic interactions in a similar manner to SPR. In combination with recent reports on multiplexed nanorod LSPR sensors³⁰ and high throughput LSPR assays,²⁰ these substrates may help to expand LSPR sensing technology more broadly.

for 1–2 min. The pale brown seed solution was stable and usable for several hours.

The nanorod growth solution was prepared by adding the following reagents to a plastic tube in the following order and then gently mixing each by inversion: 425 mL of 100 mM CTAB, 18 mL of 10 mM hydrogen tetrachloroaurate(III), and 2.7 mL of 10 mM silver nitrate (Acros, #19768). Next, 2.9 mL of 100 mM ascorbic acid (Fisher, #A61) was added and mixed by inversion, which changed the solution from brownish-yellow to colorless. To initiate nanorod growth, 1.8 mL of seed solution was added to the growth solution, mixed gently by inversion, and left still for three hours. During this time, the color changed gradually to dark purple, with most of the color change occurring in the first hour.

Gold Nanorod PEGylation. One mL of CTAB-stabilized gold nanorods was centrifuged at 7000g to pellet the nanorods. The CTAB solution was decanted, and the pellet was resuspended in 2

mM potassium carbonate. This procedure leaves sufficient CTAB in the solution that the nanorods are stable for several hours. Twenty μL of 20 mM thiol terminated methoxypoly(ethylene glycol) (mPEG-SH, 5000 MW, Nektar Therapeutics) was added to the solution and left overnight to displace the CTAB.³³ The nanorods were then taken through at least two more centrifuge/decant cycles, resuspending each time in deionized water, to further reduce the CTAB concentration.

Gold Nanorod Substrate Fabrication. Glass microscopic slides (75 mm \times 25 mm) were cleaned in piranha solution (3:1 H_2SO_4 /30% H_2O_2), thoroughly rinsed with deionized water, and dried. **WARNING: Piranha solution is very corrosive and must be handled with extreme caution; it reacts violently with organic materials.** They were then immersed in an ethanolic solution of 5 mM aminopropyltriethoxysilane (APTES) (Sigma, #440140) overnight, rinsed with water, and dried. The APTES coated slides were then immersed in a PEGylated nanorod solution overnight. Once rinsed and dried, a uniform layer of gold nanorods remained on the surface with an absorbance of approximately 0.1 at the LSPR peak wavelength. To remove the mPEG-SH and other contaminants, the substrates were processed in an oxygen plasma cleaner at low power for 30 s in 200 mT oxygen (model PDC-32G, Harrick Scientific) and immersed in an ethanolic solution of 50 μM mercaptohexadecanoic acid (Sigma, #448303) and 50 μM mercaptoundecanol (Sigma, #447528) for 2.5 h to form a mixed self-assembled monolayer (SAM). The plasma cleaning step has no significant effect on the nanorod structure as observed by atomic force microscopy and scanning electron microscopy. Plasma cleaning does cause a small LSPR blue shift consistent with the removal of a thin polymer coating.

Substrate Bioconjugation and LSPR Sensing Measurements. A closed flow cell was assembled consisting of two glass slides (one coated with nanorods covered with the mixed SAM and one clean) separated by a 1.5 mm thick polydimethylsiloxane (PDMS) seal with a 1 cm \times 2 cm slot that served as the flow volume. The clean glass slide had two drilled holes to connect the input and output flows. This flow cell was mounted vertically on an optical bench in between a quartz–tungsten–halogen light source with collimating lens and a portable spectrometer (Ocean Optics, USB 4000). The 400 $\mu\text{L}/\text{minute}$ flow rate was controlled by a syringe pump (NE1000, New Era Pump Systems).

At the start of an experiment, the substrate was exposed to 0.1 M 2-(*N*-morpholino)ethanesulfonic acid (MES) buffer (Sigma, #M-0164) at pH 6.1 until the LSPR peak wavelength stabilized. The carboxyl groups on the mixed SAM were then activated by exposure to a 1:1 mixture of 0.1 M *N*-hydroxysuccinimide (NHS) (Sigma #130672) and 0.05 M 1-ethyl-3-(3-dimethylaminopropyl)carbodiimide (EDC) (Sigma #1769) in the MES buffer, followed by rinsing in the MES buffer. Then, the substrate was exposed to rabbit IgG (Pierce, #31235) at about 1 μM in the MES buffer, followed by a rinse with 0.05 M phosphate buffered saline (PBS) with 0.25 M NaCl at pH 7.6. Finally, either goat antirabbit IgG (Pierce, #31210) or goat antimouse immunoglobulin (IgG) (Pierce, #31160) was flowed at the desired concentration in PBS buffer followed by a PBS buffer rinse. The final step could be repeated more than once for successive tests of different secondary antibodies. Absorbance spectra were averaged for 30 s and recorded. Each spectrum was then analyzed in MATLAB with a Gaussian fit to monitor the peak wavelength, height, and width versus time.

Acknowledgment. K.M. acknowledges support from the NSF-funded Integrative Graduate Research and Educational Training (IGERT) program (DGE-0750843) in nanophotonics. This work was also supported by the National Science Foundation's Nanoscale Science and Engineering Initiative under award no. EEC-018007 and EEC-0647452, the U.S. Army Research Office under grant no. W911NF-04-1-0203, the Welch Foundation under grant C-1556, and the Alliance for NanoHealth under US Army Medical Research and Material Command grant no. W81XWH-06-2-0067. The authors wish to thank Dr. Jennifer West, Dr. Rebekah Drezek, and Dr. James McNew for helpful discussions.

Supporting Information Available: Results for additional antibody–antigen kinetics experiments. This material is available free of charge via the Internet at <http://pubs.acs.org>.

REFERENCES AND NOTES

- Hutter, E.; Fendler, J. H. Exploitation of Localized Surface Plasmon Resonance. *Adv. Mater.* **2004**, *16*, 1685–1706.
- Willems, K. A.; Van Duyne, R. P. Localized Surface Plasmon Resonance Spectroscopy and Sensing. *Annu. Rev. Phys. Chem.* **2007**, *58*, 267–297.
- Karlsson, R. SPR for Molecular Interaction Analysis: A Review of Emerging Application Areas. *J. Mol. Recognit.* **2004**, *17*, 151–161.
- Fagerstam, L. G.; Frostell, A.; Karlsson, R.; Kullman, M.; Larsson, A.; Malmqvist, M.; Butt, H. Detection of Antigen–Antibody Interactions by Surface Plasmon Resonance. Application to Epitope Mapping. *J. Mol. Recognit.* **1990**, *3*, 208–214.
- Safsten, P.; Klakamp, S.; Drake, A.; Karlsson, R.; Myszyka, D. Screening Antibody–Antigen Interactions in Parallel Using Biacore A100. *Anal. Biochem.* **2006**, *353*, 181–190.
- Haes, A. J.; Van Duyne, R. P. Preliminary Studies and Potential Applications of Localized Surface Plasmon Resonance Spectroscopy in Medical Diagnostics. *Expert Review of Molecular Diagnostics* **2004**, *4*, 527–537.
- Englebienne, P. Use of Colloidal Gold Surface Plasmon Resonance Peak Shift to Infer Affinity Constants from the Interactions between Protein Antigens and Antibodies Specific for Single or Multiple Epitopes. *Analyst* **1998**, *123*, 1599–1603.
- Haes, A. J.; Van Duyne, R. P. A Nanoscale Optical Biosensor: Sensitivity and Selectivity of an Approach Based on the Localized Surface Plasmon Resonance Spectroscopy of Triangular Silver Nanoparticles. *J. Am. Chem. Soc.* **2002**, *124*, 10596–10604.
- Nath, N.; Chilkoti, A. A Colorimetric Gold Nanoparticle Sensor to Interrogate Biomolecular Interactions in Real Time on a Surface. *Anal. Chem.* **2002**, *74*, 504–509.
- Cheng, S. F.; Chau, L. K. Colloidal Gold-Modified Optical Fiber for Chemical and Biochemical Sensing. *Anal. Chem.* **2003**, *75*, 16–21.
- Frederix, F.; Friedt, J. M.; Choi, K. H.; Laureyn, W.; Campitelli, A.; Mondelaers, D.; Maes, G.; Borghs, G. Biosensing Based on Light Absorption of Nanoscaled Gold and Silver Particles. *Anal. Chem.* **2003**, *75*, 6894–6900.
- Riboh, J. C.; Haes, A. J.; McFarland, A. D.; Yonzon, C. R.; Van Duyne, R. P. A Nanoscale Optical Biosensor: Real-Time Immunoassay in Physiological Buffer Enabled by Improved Nanoparticle Adhesion. *J. Phys. Chem. B* **2003**, *107*, 1772–1780.
- Mitsui, K.; Handa, Y.; Kajikawa, K. Optical Fiber Affinity Biosensor Based on Localized Surface Plasmon Resonance. *Appl. Phys. Lett.* **2004**, *85*, 4231–4233.
- Morokoshi, S.; Ohori, K.; Mizukami, K.; Kitano, H. Sensing Capabilities of Colloidal Gold Modified with a Self-Assembled Monolayer of a Glucose-Carrying Polymer Chain on a Glass Substrate. *Langmuir* **2004**, *20*, 8897–8902.
- Nath, N.; Chilkoti, A. Label-Free Biosensing by Surface Plasmon Resonance of Nanoparticles on Glass: Optimization of Nanoparticle Size. *Anal. Chem.* **2004**, *76*, 5370–5378.
- Yonzon, C. R.; Jeoung, E.; Zou, S. L.; Schatz, G. C.; Mrksich, M.; Van Duyne, R. P. A Comparative Analysis of Localized and Propagating Surface Plasmon Resonance Sensors: The Binding of Concanavalin A to a Monosaccharide Functionalized Self-Assembled Monolayer. *J. Am. Chem. Soc.* **2004**, *126*, 12669–12676.
- Chen, H. H.; Suzuki, H.; Sato, O.; Gu, Z. Z. Biosensing Capability of Gold-Nanoparticle-Immobilized Three-Dimensionally Ordered Macroporous Film. *Appl. Phys., A: Mater. Sci. Process.* **2005**, *81*, 1127–1130.
- Endo, T.; Yamamura, S.; Nagatani, N.; Morita, Y.; Takamura, Y.; Tamiya, E. Localized Surface Plasmon Resonance Based Optical Biosensor Using Surface Modified Nanoparticle

- Layer for Label-Free Monitoring of Antigen-Antibody Reaction. *Sci. Technol. Adv. Mater.* **2005**, *6*, 491–500.
19. Kalele, S. A.; Ashtaputre, S. S.; Hebalkar, N. Y.; Gosavi, S. W.; Deobagkar, D. N.; Deobagkar, D. D.; Kulkarni, S. K. Optical Detection of Antigen-Antibody Reaction Using Silica-Silver Core-Shell Particles. *Chem. Phys. Lett.* **2005**, *404*, 136–141.
 20. Endo, T.; Kerman, K.; Nagatani, N.; Hiepa, H. M.; Kim, D. K.; Yonezawa, Y.; Nakano, K.; Tamiya, E. Multiple Label-Free Detection of Antigen-Antibody Reaction Using Localized Surface Plasmon Resonance-Based Core-Shell Structured Nanoparticle Layer Nanochip. *Anal. Chem.* **2006**, *78*, 6465–6475.
 21. Fujiwara, K.; Watarai, H.; Itoh, H.; Nakahama, E.; Ogawa, N. Measurement of Antibody Binding to Protein Immobilized on Gold Nanoparticles by Localized Surface Plasmon Spectroscopy. *Anal. Bioanal. Chem.* **2006**, *386*, 639–644.
 22. Kitano, H.; Anraku, Y.; Shinohara, H. Sensing Capabilities of Colloidal Gold Monolayer Modified with a Phenylboronic Acid-Carrying Polymer Brush. *Biomacromolecules* **2006**, *7*, 1065–1071.
 23. Kreuzer, M. P.; Quidant, R.; Badenes, G.; Marco, M. P. Quantitative Detection of Doping Substances by a Localised Surface Plasmon Sensor. *Biosens. Bioelectron.* **2006**, *21*, 1345–1349.
 24. Stewart, M. E.; Mack, N. H.; Malyarchuk, V.; Soares, J. A. N. T.; Lee, T. W.; Gray, S. K.; Nuzzo, R. G.; Rogers, J. A. Quantitative Multispectral Biosensing and 1D Imaging Using Quasi-3D Plasmonic Crystals. *Proc. Natl. Acad. Sci. U.S.A.* **2006**, *103*, 17143–17148.
 25. Arai, T.; Kumar, P.; Rockstuhl, C.; Awazu, K.; Tominaga, J. An Optical Biosensor Based on Localized Surface Plasmon Resonance of Silver Nanostructured Films. *J. Opt., A* **2007**, *9*, 699–703.
 26. Chen, C. D.; Cheng, S. F.; Chau, L. K.; Wang, C. R. C. Sensing Capability of the Localized Surface Plasmon Resonance of Gold Nanorods. *Biosens. Bioelectron.* **2007**, *22*, 926–932.
 27. Gish, D.; Nsiah, F.; McDermott, M.; Brett, M. Localized Surface Plasmon Resonance Biosensor Using Silver Nanostructures Fabricated by Glancing Angle Deposition. *Anal. Chem.* **2007**, *79*, 4228–4232.
 28. Marinakos, S. M.; Chen, S. H.; Chilkoti, A. Plasmonic Detection of a Model Analyte in Serum by a Gold Nanorod Sensor. *Anal. Chem.* **2007**, *79*, 5278–5283.
 29. Miller, M. M.; Lazarides, A. A. Sensitivity of Metal Nanoparticle Surface Plasmon Resonance to the Dielectric Environment. *J. Phys. Chem. B* **2005**, *109*, 21556–21565.
 30. Yu, C. X.; Irudayaraj, J. Multiplex Biosensor Using Gold Nanorods. *Anal. Chem.* **2007**, *79*, 572–579.
 31. Haes, A. J.; Chang, L.; Klein, W. L.; Van Duyne, R. P. Detection of a Biomarker for Alzheimer's Disease from Synthetic and Clinical Samples Using a Nanoscale Optical Biosensor. *J. Am. Chem. Soc.* **2005**, *127*, 2264–2271.
 32. Lin, T. J.; Huang, K. T.; Liu, C. Y. Determination of Organophosphorous Pesticides by a Novel Biosensor Based on Localized Surface Plasmon Resonance. *Biosens. Bioelectron.* **2006**, *22*, 513–518.
 33. Liao, H.; Hafner, J. Gold Nanorod Bioconjugates. *Chem. Mater.* **2005**, *17*, 4636–4641.
 34. Sau, T. K.; Murphy, C. J. Room Temperature, High-Yield Synthesis of Multiple Shapes of Gold Nanoparticles in Aqueous Solution. *J. Am. Chem. Soc.* **2004**, *126*, 8648–8649.
 35. Nikoobakht, B.; El-Sayed, M. A. Preparation and Growth Mechanism of Gold Nanorods (NRs) Using Seed-Mediated Growth Method. *Chem. Mater.* **2003**, *15*, 1957–1962.
 36. Hermanson, G. T. *Bioconjugate Techniques*, 1st ed.; Academic Press: San Diego, CA, 1996; Vol. 16, pp 9–177.
 37. Gao, J. X.; Bender, C. M.; Murphy, C. J. Dependence of the Gold Nanorod Aspect Ratio on the Nature of the Directing Surfactant in Aqueous Solution. *Langmuir* **2003**, *19*, 9065–9070.
 38. Lahiri, J.; Isaacs, L.; Tien, J.; Whitesides, G. M. A Strategy for the Generation of Surfaces Presenting Ligands for Studies of Binding Based on an Active Ester as a Common Reactive Intermediate: A Surface Plasmon Resonance Study. *Anal. Chem.* **1999**, *71*, 777–790.
 39. Hostetler, M. J.; Wingate, J. E.; Zhong, C. J.; Harris, J. E.; Vachet, R. W.; Clark, M. R.; Londono, J. D.; Green, S. J.; Stokes, J. J.; Wignall, G. D.; Glish, G. L.; Porter, M. D.; Evans, N. D.; Murray, R. W. Alkanethiolate Gold Cluster Molecules with Core Diameters from 1.5 to 5.2 nm: Core and Monolayer Properties as a Function of Core Size. *Langmuir* **1998**, *14*, 17–30.
 40. Liao, H.; Nehl, C. L.; Hafner, J. H. Biomedical Applications of Plasmon Resonant Metal Nanoparticles. *Nanomedicine* **2006**, *1*, 201–208.
 41. Sherry, L. J.; Chang, S.-H.; Schatz, G. C.; van Duyne, R. P. Localized Surface Plasmon Resonance Spectroscopy of Single Silver Nanocubes. *Nano Lett.* **2005**, *5*, 2034–2038.
 42. Malinsky, M. D.; Kelly, K. L.; Schatz, G. C.; Van Duyne, R. P. Nanosphere Lithography: Effect of Substrate on the Localized Surface Plasmon Resonance Spectrum of Silver Nanoparticles. *J. Phys. Chem. B* **2001**, *105*, 2343–2350.
 43. Davies, C. Introduction to Immunoassay Principles. *The Immunoassay Handbook*, 3rd ed.; Wild, D., Ed.; Elsevier: Amsterdam, The Netherlands, 2005; pp 3–40.
 44. Wang, H.; Brandl, D. W.; Le, F.; Nordlander, P.; Halas, N. J. Nanorice: A Hybrid Plasmonic Nanostructure. *Nano Lett.* **2006**, *6*, 827–832.
 45. Bukasov, R.; Shumaker-Parry, J. S. Highly Tunable Infrared Extinction Properties of Gold Nanocrescents. *Nano Lett.* **2007**, *7*, 1113–1118.
 46. Henzie, J.; Lee, M. H.; Odom, T. W. Multiscale Patterning of Plasmonic Metamaterials. *Nat. Nanotechnol.* **2007**, *2*, 549–554.